Acta Pharmacologica Sinica (2016) 37: 1337–1348
 1671-4083/16
www.nature.com/aps

Original Article

Betulin attenuates atherosclerosis in apoE$^{-/-}$ mice by up-regulating ABCA1 and ABCG1

Yu-zhou GUI[1, 2], Hong YAN[1, 2], Fei GAO[1, 2], Cong XI[1, 2], Hui-hui LI[1, 2], Yi-ping WANG[1, 2, *]

[1]*University of Chinese Academy of Sciences, Beijing 100049, China;* [2]*State Key Laboratory of Drug Research, Shanghai Institute of Materia Medica, Chinese Academy of Sciences, Shanghai 201203, China*

Aim: Betulin is a pentacyclic triterpenoid isolated from the bark of yellow and white birch trees with anti-cancer and anti-malaria activities. In this study we examined the effects of betulin on atherosclerosis in apoE$^{-/-}$ mice and the underlying mechanisms.
Methods: Murine macrophage RAW264.7 cells and human monocyte-derived THP-1 cells were tested. Foam cell formation was detected with Oil Red O staining. Cholesterol efflux was assessed using [^{3}H]-cholesterol efflux assay. The expression of ATP-binding cassette transporter A1 and G1 (ABCA1 and ABCG1) was examined using RT-PCR and Western-blotting. The ABCA1 promoter activity was evaluated using luciferase activity assay. Male apoE$^{-/-}$ mice fed on a high-fat-diet (HFD), and received betulin (20 and 40 mg·kg^{-1}·d^{-1}, ig) for 12 weeks. The macrophage content and ABCA1 expression in the aortic sinuses were evaluated with immunofluorescence staining. The hepatic, intestinal and fecal cholesterol were also analyzed in the mice.
Results: In RAW264.7 cells, betulin (0.1–2.5 μg/mL) dose-dependently ameliorated oxLDL-induced cholesterol accumulation and enhanced cholesterol efflux. In both RAW264.7 and THP-1 cells, betulin increased the expression of ABCA1 and ABCG1 via suppressing the transcriptional repressors sterol-responsive element-binding proteins (SREBPs) that bound to E-box motifs in ABCA1 promoter, whereas E-box binding site mutation markedly attenuated betulin-induced ABCA1 promoter activity. In HFD-fed apoE$^{-/-}$ mice, betulin administration significantly reduced lesions in *en face* aortas and aortic sinuses. Furthermore, betulin administration significantly increased ABCA1 expression and suppressed macrophage positive areas in the aortic sinuses. Moreover, betulin administration improved plasma lipid profiles and enhanced fecal cholesterol excretion in the mice.
Conclusion: Betulin attenuates atherosclerosis in apoE$^{-/-}$ mice by promoting cholesterol efflux in macrophages.

Keywords: atherosclerosis; macrophage; betulin; atorvastatin; T0901317; 25-OH cholesterol; ATP-binding cassette transporter A1; ATP-binding cassette transporter G1; sterol-responsive element-binding protein

Acta Pharmacologica Sinica (2016) 37: 1337–1348; doi: 10.1038/aps.2016.46; published online 4 Jul 2016

Introduction

Foam cell formation, due to excessive cholesterol accumulation in macrophages, is recognized as the initial step and hallmark in the development of atherosclerosis[1]. Although there has been great effort to alleviate cholesterol overload in macrophages, the current situation is far from satisfactory. Excessive cholesterol can be removed from peripheral macrophages and returned to the liver for metabolism and excretion in the feces, which is called reverse cholesterol transport (RCT)[2]. Cholesterol efflux is the first step in RCT, which is mediated by a group of membrane transporters, including ATP-binding cassette transporter A1 and G1 (ABCA1 and ABCG1)[3, 4].

ABCA1 mediates the efflux of cholesterol and phospholipids to lipid-poor apolipoprotein A-I (apoA-I), while ABCG1 induces cholesterol efflux to HDL particles[5]. ABCA1 mutations in humans result in defective cellular efflux of phospholipids and cholesterol[6, 7], severe reductions in plasma HDL levels and increased susceptibility to atherosclerosis[8]. Overexpression of ABCA1 in C57BL/6 mice leads to significantly lower aortic atherosclerosis[9]. In particular, bone marrow transplantation of ABCA1-KO mice with wild type macrophages[10] or macrophages that specifically over-express ABCA1[11] resulted in a substantial decrease in atherosclerosis. The combined deficiency of ABCA1 and ABCG1 promotes foam cell accumulation and accelerates atherosclerosis in mice[12]. Therefore, up-regulation of ABCA1 and ABCG1 has been proposed as a therapeutic target in treating atherosclerosis.

The regulatory element in the ABCA1 promoter has been mapped to a region containing the E-box motif[13]. Deletion

*To whom correspondence should be addressed.
E-mail ypwang@mail.shcnc.ac.cn
Received 2016-02-01 Accepted 2016-04-28

of the E-box motif in the ABCA1 promoter causes a 3-fold increase in transcriptional activity under basal conditions[14]. Sterol-responsive element-binding protein 2 (SREBP2) represses basal ABCA1 expression through the E-box motif that is upstream of the ABCA1 transcriptional start site[15]. In addition, ABCA1 is transcriptionally regulated by the liver X receptor (LXR). Oxysterols, such as 22(R)-OH cholesterol[16], and non-steroidal-LXR agonists, such as GW3965[17] and T0901317[18], are reported to up-regulate ABCA1 gene promoter activity.

Betulin is a pentacyclic triterpenoid natural product isolated from the bark of yellow and white birch trees[19] with a wide range of pharmacological properties, such as anti-cancer and anti-malaria activities[20]. Initial studies have also shown that betulin significantly suppresses atherosclerosis in mice[21], but the underlying mechanisms of this effect remain elusive.

The aim of the current study was to demonstrate the effects of betulin on atherosclerosis in apoE-deficient mice and to explore the underlying mechanisms of these effects. Our results showed that long-term administration of betulin significantly suppressed atherosclerosis in apoE$^{-/-}$ mice. Mechanistically, betulin induced ABCA1/ABCG1-mediated cholesterol efflux in macrophages *via* the E-box motif and SREBPs. These results suggest that betulin may be a promising new compound with therapeutic potential in atherosclerosis.

Materials and methods

Chemicals and reagents

Betulin (purity >98%) was purchased from Dalian Meilun Biology Technology Co, Ltd (Dalian, Liaoning, China). Dulbecco's modified Eagle's medium (DMEM) and RPMI-1640 medium were purchased from HyClone Laboratories (Logan, Utah, USA). Fetal bovine serum (FBS) and Lipofectamine 3000 transfection reagent were obtained from ThermoFisher Scientific (Carlsbad, California, USA). Phorbol 12-myristate 13-acetate (PMA), Oil Red O, atorvastatin and T0901317 were purchased from Sigma-Aldrich (St Louis, MI, USA).

Cell cultures

Murine peritoneal macrophage cell line RAW264.7 cells were grown in DMEM containing 10% (*v/v*) fetal bovine serum (FBS). Human monocyte-derived THP-1 cells were maintained in RPMI-1640 supplemented with 10% (*v/v*) FBS. Monocytic THP-1 cells were incubated with 100 nmol/L PMA for 24 h to differentiate them into adherent macrophages. Then, the culture was replaced with complete RPMI-1640 supplemented with 10% FBS. Adherent macrophages were cultured for another 24 h before treatment.

Lipoprotein isolation and modification

Human plasma was obtained from Shanghai Xuhui Central Hospital, China, after the receipt of informed consent and with the approval of the local ethics committee. The use of human plasma in this study conformed to the principles outlined in the Declaration of Helsinki[22]. Human LDL (d=1.019–l.063 g/mL) and HDL (d=1.1–l.21 g/mL) were separated from fresh plasma by ultra-centrifugation[23]. Oxidation was performed by incubation of LDL with 2 mmol/L $CuSO_4$ at 37 °C for 24 h. The extent of LDL oxidation was evaluated by measuring the formation of thiobarbituric acid-reacting substances (TBARS). Protein concentrations were determined using the BCA Protein Assay Kit (Beyotime Biotechnology, China). All lipoproteins were sterilized by filtration through a 0.22-μm filter and stored at 4 °C in the dark before use.

Foam cell assay

Foam cell formation was evaluated by Oil Red O staining. In brief, cells were co-incubated with ox-LDL (20 μg/mL) alone or combined with betulin (0.1, 0.5, 2.5 μg/mL) in DMEM for 24 h. At the end of the treatment, cells were fixed with 4% paraformaldehyde and then stained with filtered 0.5% Oil Red O (ORO). Images were obtained from at least three randomly selected fields for each condition using DP70 microscopy (Olympus, Japan). Staining areas were utilized to determine total lipid content. Positive Oil Red O areas were determined by Image-Pro Plus 6.0 software (Media Cybernetics Inc, USA).

Cholesterol efflux assay

RAW264.7 cells were plated into 24-well plates (Corning, USA) at a density of 1×10^6 cells/mL and labeled with labeling medium (DMEM) containing 0.2% BSA, 20 μg/mL oxLDL and 1 μCi/mL [^{3}H]-cholesterol (Perkin Elmer Life Sciences, USA). After 24 h of labeling, the cells were washed twice with PBS and incubated with or without betulin (0.1, 0.5 and 2.5 μg/mL) in 0.2% BSA, serum-free DMEM medium for 24 h. At the end of the treatment period, cells were washed twice with PBS and incubated with 0.2% BSA serum-free DMEM medium with or without purified apoA-I (20 μg/mL) or human HDL (20 μg/mL). After incubation for 3 h, the culture medium was centrifuged to remove cell debris, and the cells were washed and lysed using 500 μL of 0.2 mol/L NaOH for 5 min. Cell lysates were harvested and centrifuged for 2 min. The supernatant of the cell lysate and culture medium were counted separately by liquid scintillation (Perkin Elmer Life Sciences, USA). The percentage of [^{3}H]-cholesterol efflux was calculated as the percentage of [^{3}H]-cholesterol counts in the medium compared with the total [^{3}H]-cholesterol counts in the supernatant and cell lysate[24].

RNA isolation and real-time PCR

The total RNA of RAW264.7, THP-1 and HepG2 cells was extracted using TRIzol reagent, according to the manufacturer's instructions, and the RNA was converted into cDNA by reverse transcriptase (Takara, China). Total RNA was also extracted from the liver tissues of apoE$^{-/-}$ mice using the same method. The primers are listed in Table 1. Real-time quantitative PCR was performed with a CFX Real-Time PCR Detection System (Bio-Rad, USA) using SYBR Green PCR Supermixes (Bio-Rad, USA) and specific primers. Quantification of relative gene expression was performed with the efficiency-corrected $2^{-\triangle\triangle CT}$ method[25], and the housekeeping gene GAPDH was used as the internal control. The data are presented as the fold

Table 1. Primer sequences for real-time quantitative PCR.

Genes	Forward primer 5′ to 3′	Reverse primer 5′ to 3′
hABCA1	CTGAAGCCAATCCTGAGAACAC	CCGCAGACAATACGAGACAC
hABCG1	GGTGATGCCGAGGTGAAC	CAATGTGCGAGGTGATGC
hCD36	CCTCCTTGGCCTGATAGAAA	GTTTGTGCTTGAGCCAGGTT
hLDLR	CTGAAATCGCCGTGTTACTG	GCCAATCCCTTGTGACATCT
hFAS	AAGGACCTGTCTAGGTTTGATGC	TGGCTTCATAGGTGACTTCCA
hACC	GAGGGCTAGGTCTTTCTGGAAG	CCACAGTGAAATCTCGTTGAGA
hHMG-CR	GTCATTCCAGCCAAGGTTGT	GGGACCACTTGCTTCCATTA
hGAPDH	AAGAAGGTGGTGAAGCAGG	AGGTGGAGGAGTGGGTGTCG
mABCA1	ACTTAGGGCACAATTCCACAAGA	CTCCTGTGGTGTTTCTGGATGA
mABCG1	TCACCCAGTTCTGCATCCTCTT	GCAGATGTGTCAGGACCGAGT
mCD36	GGAGTGCTGGATTAGTGGTTAG	GCTGTGAGCAGACGTATAGAAG
mLDLR	AGGCTGTGGGCTCCATAGG	TGCGGTCCAGGGTCATC
mFAS	GCTGCGGAAACTTCAGGAAAT	AGAGACGTGTCACTCCTGGACTT
mACC	TGACAGACTGATCGCAGAGAAAG	TGGAGAGCCCCACACACA
mHMG-CR	CTTGTGGAATGCCTTGTGATTG	AGCCGAAGCAGCACATGAT
mGAPDH	GTGTGAACGGATTTGGCCGT	GACAAGCTTCCCATTCTCGG

change over the control group.

Western blotting analysis

Nuclear protein and cytosolic protein were extracted using the Nuclear and Cytoplasmic Protein Extraction Kit (Beyotime Biotechnology, China), respectively. Total cell protein was extracted with RIPA Lysis Buffer (Beyotime Biotechnology, China). The Protease Inhibitor Cocktail Set (Merck Millipore, Germany) was added to protect proteins from degradation. Each sample containing equal amounts of protein (40 μg) was separated by 7%–12% SDS-PAGE and electro-transferred onto a polyvinylidene difluoride membrane (Bio-Rad, USA). The primary antibodies used for Western blotting were ABCA1 (AB18180, 1:500, Abcam), CD36 (GTX100642, 1:500, Genetex), ABCG1 (GTX108934, 1:1000, Genetex), LXRα (GTX113912, 1:500, Genetex), LXRβ (GTX113571, 1:500, Genetex), anti-GAPDH (2118, 1:2000, CST) and anti-β-actin (a1978, 1:2000, Sigma). The immunoreactive signal was detected by an enhanced chemiluminescence detection kit (Bio-Rad, USA). The band intensities were quantified using Quantity One analysis software (Bio-Rad, USA).

Construction of ABCA1 promoter-driven luciferase reporter plasmids

Plasmids expressing luciferase under ABCA1 promoter sequences were used to determine the effect of betulin at the transcriptional level. The mouse ABCA1 promoter sequence (-250/-1 bp) was amplified by PCR using the following primers (forward 5′-TGCCTCGAGGGCCAGGGCTACAGAAAGCGG-3′ and reverse 5′-CCGAAGCTTGGTTTTTGCCGCGACTAGTTC-3′). The restriction sites are underlined. The resulting PCR fragment containing the ABCA1 promoter sequence was digested with *Xho* I and *Hin*d III restriction enzymes and cloned into the *Xho* I/*Hin*d III restriction sites of the luciferase reporter plasmid pGL3-basic vector (Promega, USA). The mutations of the E-box and LXR sites in the ABCA1 promoter were constructed using an overlap PCR method with the QuikChange Lightning Site Directed Mutagenesis Kit (Agilent, USA), according to the manufacturer's instructions. The overlap PCR primers were as follows: mE-box (forward 5′-GGGCGGGCCATGTCTCCAaaTGCTTTCTGCTGAGTGAC-3′ and reverse 5′-GTCACTCAGCAGAAAGCAttTGGAGACATGGCCCGCCC-3′) and mLXR (forward 5′-GGGAGAGAACAGCGTTTGtgtGGTAGTAACtaCGGCGCTCGGCAC-3′ and reverse 5′-GTGCCGAGCGCCGtaGTTACTACCacaCAAACGCTGTTCTCTCCC-3′). Uppercase letters represent the wild-type sequence, and lower-case letters represent the mutant sequence. All of the constructs were confirmed by sequencing.

Transfection and luciferase assay

Murine RAW264.7 cells, at a density of 1×10^5 cells/mL, were plated in 12-well plates (Corning, USA), grown to 40%–60% confluency and co-transfected with 1 μg of the ABCA1 promoter-luciferase plasmid (wild-type, E-box mutant or LXR mutant) and 0.5 μg of pRL-null *Renilla* plasmid as an internal control in serum-free DMEM using Lipofectamine 3000 reagents (ThermoFisher Scientific, USA). Six hours after the addition of the plasmid, the cells were maintained in fresh DMEM containing 10% FBS and incubated for another 18 h at 37 °C. Following transfection, cells were treated with betulin (2.5 μg/mL) for 24 h. Then, the cells were lysed, and the cell lysates were harvested by centrifugation at 13 000×*g* for 2 min. Luciferase activity was measured using the Dual-Luciferase Reporter Assay System (Promega, USA), according to the manufacturer's protocol. The ratio of firefly luciferase activity in relative light units was divided by *Renilla* luciferase activity to give a normalized luciferase value.

Mice and lipid analysis

Male apoE$^{-/-}$ mice (6 week-old, SPF class, C57BL/6J background, provided by the Animal Center of Shanghai Institute of Materia Medica) were kept under constant temperature and humidity under a 12 h controlled dark/light cycle. Mice were administered carboxymethylcellulose sodium (CMC-Na), atorvastatin (10 mg/kg) or betulin [20 and 40 mg/kg as BT (L) and BT (H), respectively] intragastrically (ig) daily while being fed a high fat diet (HFD) (0.15% cholesterol and 18% fat) for 12 weeks. Mice on a chow diet served as the negative control group and received CMC-Na. Body weight and food intake were monitored.

Animal experiments were conducted according to the National Research Council's guidelines. All of the experimental protocols and procedures were approved by the Institutional Ethical Committee of Shanghai Institute of Materia Medica.

Analysis of atherosclerotic lesions

After 12 weeks of treatment, apoE$^{-/-}$ mice were euthanized and perfused with cold 0.01 mol/L PBS through the left ventricle. Aortas were dissected from the proximal ascending aorta to the bifurcation of the iliac artery and fixed in 4% buffered paraformaldehyde for 24 h. After fixation, the aortas were split longitudinally and pinned open for surface lesion measurements with 1% Sudan IV staining for 10 min. Images of the stained aortas were analyzed with Image-Pro Plus 6.0 software to quantify the lesion areas. For aortic sinus analysis, the heart was embedded in optimal cutting temperature compound (OCT), and snap-frozen in liquid nitrogen. Serial 7-μm cryosections of the aortic sinus were cut using a Leica CM1950 cryostat and collected from the aortic region moving toward the apex of the heart and sequentially placed on slides. Cryosections were fixed in 4% buffered paraformaldehyde and stained in 0.5% Oil Red O for 25 min. Images of the stained sections were obtained via DP70 microscopy (Olympus, Japan). Lesion areas were quantified using Image-Pro Plus 6.0 software.

Immunofluorescence study

To evaluate effects of betulin on macrophage content and ABCA1 expression in the aortic sinus, frozen sections were incubated with rabbit anti Mac-2 antibody (Santa Cruz Biotechnology; dilution 1:50) and mouse anti ABCA1 antibody (Abcam; dilution 1:50) at 4 °C overnight, followed by Dylight Fluor594-conjugated anti-rabbit IgG (H+L) secondary antibody and Dylight Fluor488-conjugated anti-mouse IgG (H+L) secondary antibody (Jackson Immunoresearch Laboratories; 1:100) for 1 h at room temperature. Slides were counterstained with DAPI (50 μg/mL, Sigma), mounted in glycerin jelly medium, and subjected to confocal microscopy (Olympus, Japan). The immunofluorescence intensities of ABCA1 and Mac-2 were quantified by Image-Pro Plus 6.0 software.

Plasma, liver, intestine and fecal cholesterol analysis

At the end of treatment, all of the mice were fasted overnight (12 h) before blood samples were collected from the retro-orbital plexus. Plasma total cholesterol (TC), LDL cholesterol (LDL-C) and triglyceride (TG) levels were measured using an automatic analyzer (Hitachi, Japan).

During the last day of treatment, we collected 24 h of feces from the cages of each group. On the last day of treatment, the liver and intestine were harvested. The feces were dried before being frozen and stored at -80 °C. The liver and intestine were snap-frozen in liquid nitrogen and stored at -80 °C. Total cholesterol in the liver, intestine or feces was extracted by using a published method and measured with an automatic analyzer (Hitachi, Japan)[26].

Statistical analysis

Statistical calculations were performed using GraphPad Prism, Version 5. Comparisons between groups were performed using Student's *t*-test. For multiple comparisons, the data were analyzed using one-way analysis of covariance (ANOVA) with a Dunnett *post-hoc* test.

The data are expressed as the mean±SEM of at least three independent experiments unless otherwise specified. Differences were considered to be statistically significant when $P<0.05$.

Results

Betulin attenuates foam cell formation by promoting cholesterol efflux *in vitro*

We first investigated the effect of betulin on foam cell formation. Ox-LDL (20 μg/mL) treatment significantly induced foam cell formation in RAW264.7 cells, which was characterized by increased lipid storage in the cytoplasm. T0901317 significantly alleviated cholesterol accumulation in RAW264.7 cells (Figure 1A and 1B) ($P<0.01$). Betulin (0.1, 0.5, and 2.5 μg/mL) markedly attenuated intracellular lipid accumulation (Figure 1A and 1B). ORO-positive areas were reduced by 16.7%±7.4%, 34.9%±8.1%, and 40.7%±6.1% in the betulin treated groups (0.1, 0.5, and 2.5 μg/mL) ($P<0.01$).

We then evaluated the effects of betulin on cholesterol efflux. As shown in Figure 1C and 1D, the positive control, T0901317, significantly induced cholesterol efflux in RAW264.7 cells (Figure 1C and 1D) ($P<0.05$). Betulin (0.1, 0.5, and 2.5 μg/mL) significantly enhanced cholesterol efflux to extracellular apoA-I and HDL, with maximal 4.2- ($P<0.01$) and 3.0-fold changes ($P<0.01$), respectively. Taken together, these data clearly suggest that betulin ameliorates the formation of macrophage foam cells by promoting apoA-I and HDL-mediated cholesterol efflux.

Betulin promotes ABCA1 and ABCG1 expression *in vitro*

ABCA1 and ABCG1 are mainly responsible for cholesterol efflux in macrophages. As shown in Figure 2A and 2C, betulin enhanced ABCA1 and ABCG1 mRNA levels in a dose-dependent manner in both RAW264.7 cells and THP-1 cells, with the greatest induction at 2.5 μg/mL. Western blotting analysis in RAW264.7 cells revealed that betulin markedly up-regulated ABCA1 and ABCG1 protein levels by 10- and 1.9-fold, respec-

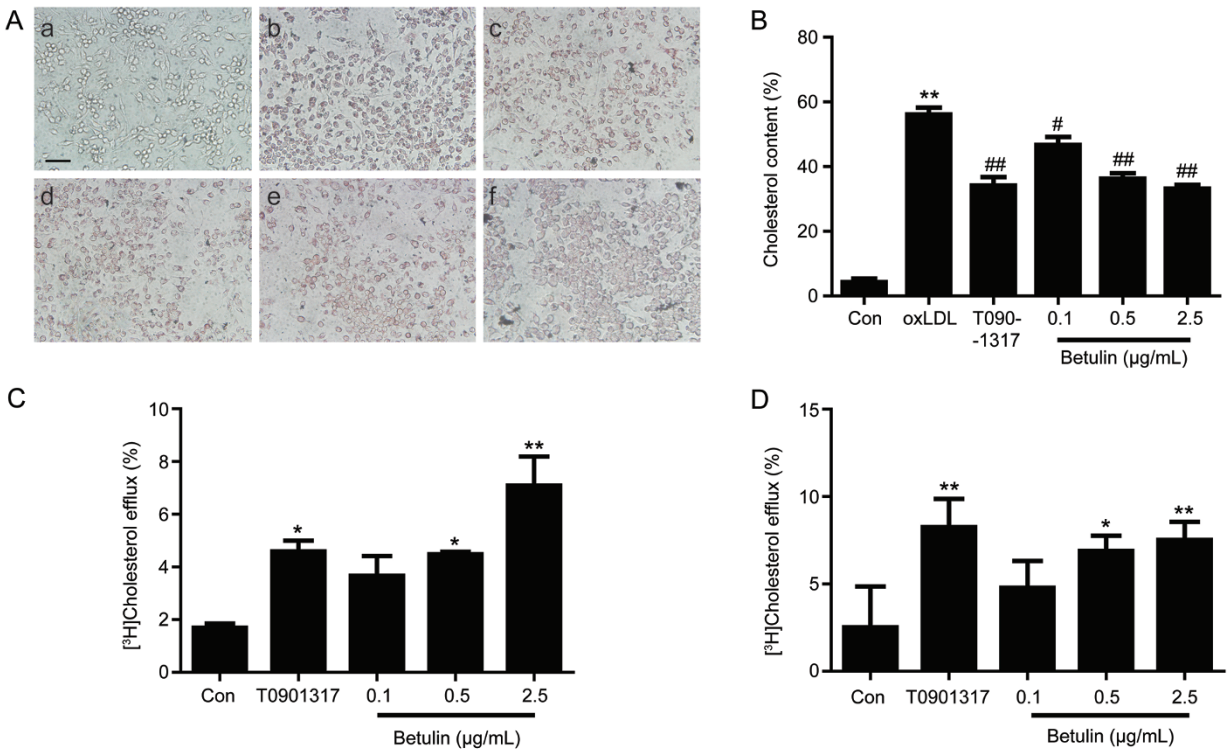

Figure 1. Betulin ameliorates lipid accumulation in RAW264.7 macrophages by increasing cholesterol efflux *in vitro*. (A) Foam cell formation was determined by Oil Red O staining. (a: control; b: oxLDL 20 μg/mL; c: T0901317 1 μmol/L; d–f: betulin 0.1, 0.5, and 2.5 μg/mL). (B) ORO areas were calculated as percentages of the stained cell area to the total cell area. The data are presented as the mean±SEM of three independent experiments. $^{**}P<0.01$ *vs* Control. $^{\#}P<0.05$, $^{\#\#}P<0.01$ *vs* ox-LDL group. Magnification is ×100. (C, D) Cholesterol efflux was evaluated by incubating with apoA-I (20 μg/mL) (C) or human HDL (20 μg/mL) (D) and calculated as a percentage of the radioactivity in the supernatant to the total radioactivity in the supernatant and cell lysates. Con: vehicle; T0901317: T0901317 1 μmol/L. The data are presented as the mean±SEM of three independent experiments and expressed as the absolute efflux rate. $^{*}P<0.05$, $^{**}P<0.01$ *vs* control. Scale bar=2.5 μm.

tively (Figure 2B). In addition, betulin enhanced ABCA1 and ABCG1 protein levels markedly in THP1 cells (Figure 2D).

Recent studies indicate that CD36, a member of the scavenger receptor B family, mediates the uptake of oxidized LDL and subsequently affects cellular cholesterol homeostasis in macrophages[27]. Therefore, the effect of betulin on CD36 was also examined. As shown in Figure 1A and 1C, betulin had no effect on CD36 mRNA levels in RAW264.7 cells and THP-1 cells. Western blotting analysis further confirmed that the protein expression of CD36 in RAW264.7 (Figure 1B) and THP1 cells (Figure 1D) was not affected by betulin. These data suggest that betulin enhances the expression of cholesterol transporters, such as ABCA1 and ABCG1, and does not affect the expression of CD36 in both murine and human macrophages.

Betulin promotes ABCA1 expression by inhibiting SREBP processing

The results shown in Figure 2A and 2C indicate that betulin regulated ABCA1 expression at the transcription level. To define the betulin-responsive region within the ABCA1 promoter, we generated luciferase reporter constructs of the mouse ABCA1 promoter. Various binding motifs in the proximal -250 bp of the mouse ABCA1 promoter have been identified, including those for Sp1 (-100 and -166 bp), AP1 (-131 bp), LXR (-69 bp), and E-box (-147 bp)[13], and among them, the LXR and E-box motifs are known as crucial transcription regulatory sites in the ABCA1 promoter[14, 16]. Therefore, LXR and E-box mutations were introduced in the ABCA1 promoter. Mutation of the E-box site markedly increased basal promoter activity, while mutation of the LXR binding site significantly suppressed basal promoter activity compared with the wild type ABCA1 promoter (Figure 3A). Betulin-induced ABCA1 promoter activity was markedly abrogated by the E-box mutation ($P<0.01$), but not by the LXR mutation (Figure 3A), suggesting that betulin regulated ABCA1 by activating E-box motif binding proteins.

Based on the fact that sterol-responsive element-binding proteins (SREBPs) are major transcriptional repressors binding to E-box motifs[15], we investigated nuclear and cytosolic SREBP protein expression in RAW264.7 macrophage cells. 25-OH cholesterol had two major effects on the nuclear proteins: decreasing nuclear SREBP2 protein levels and activating LXR, which leads to the induction of nuclear SREBP1 protein levels (Figure 3B). As shown in Figure 3B, betulin (0.1, 0.5, and 2.5 μg/mL) significantly suppressed the nuclear SREBP proteins, but the cytosol precursor SREBP proteins remained

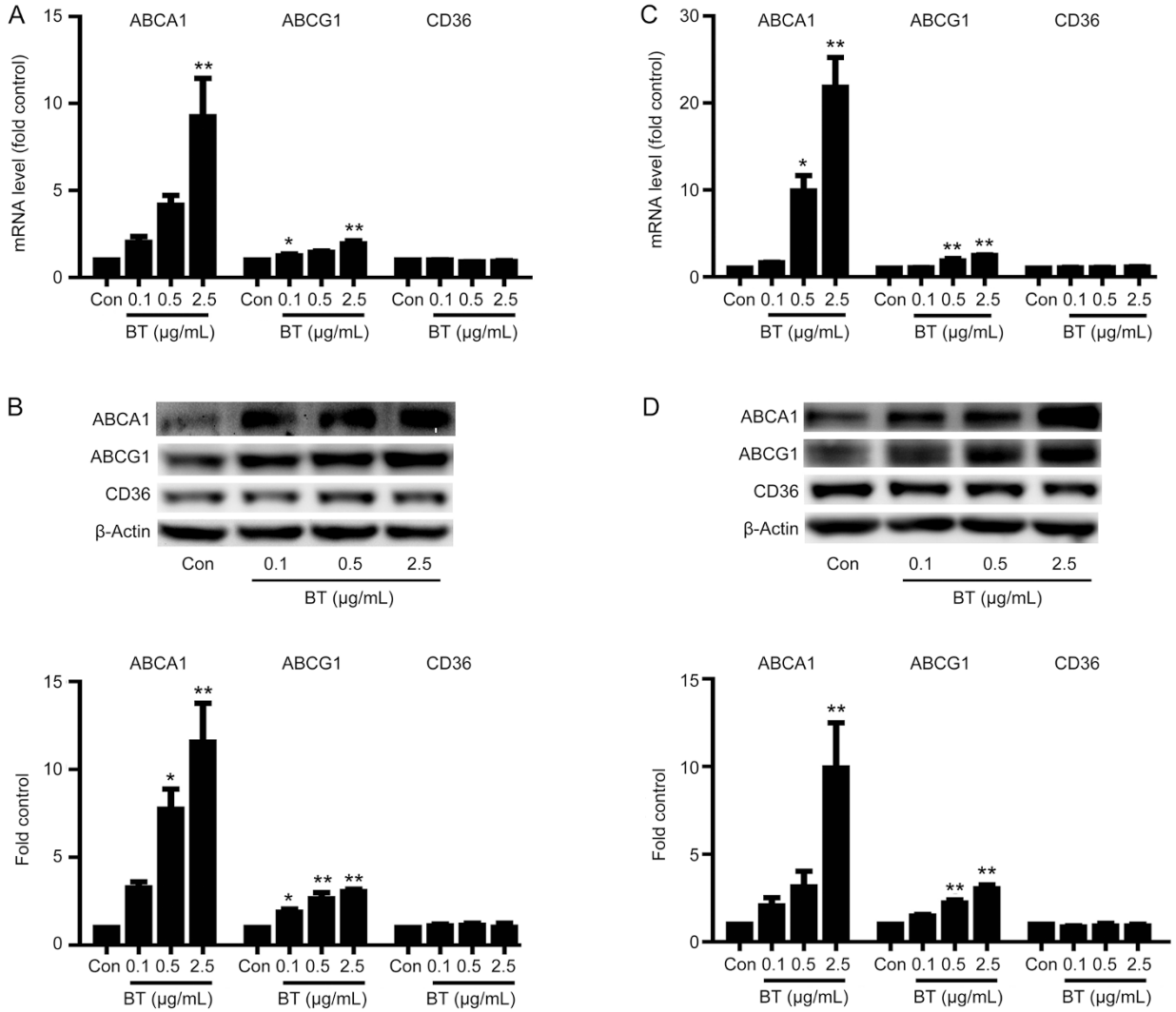

Figure 2. Betulin regulates ABCA1 and ABCG1 expression *in vitro*. The mRNA levels of the indicated genes in RAW264.7 cells (A) and THP-1 cells (C) were determined using real-time PCR. The protein levels in RAW264.7 cells (B) and THP-1 cells (D) were determined via Western blotting analysis. Representative Western blotting images of proteins from RAW264.7 cells (B) and THP-1 cells (D) are shown. Protein abundance was normalized to that of β-actin. The data are expressed as the mean±SEM of three independent experiments, relative to the control. $^{*}P<0.05$, $^{**}P<0.01$ *vs* control.

stable, which indicated that betulin suppressed SREBP intracellular processing.

To further determine the effect of betulin on SREBPs, we investigated the mRNA expression of several SREBP target genes. As shown in Figure 3C, betulin significantly inhibited the mRNA expression of HMG-CR, LDLR, ACC, and FAS in RAW264.7 cells ($P<0.05$). Similar results were observed in HepG2 cells and in the liver tissues of apoE$^{-/-}$ mice (Figure S1). Betulin significantly inhibited the mRNA expression of SREBP target genes, such as LDLR, FAS, and HMG-CR, in HepG2 cells ($P<0.05$). Compared with the model group, betulin (30 mg/kg) significantly inhibited the mRNA expression of the following SREBP target genes: LDLR, FAS, ACC, and HMG-CR, in the liver tissues of apoE$^{-/-}$ mice ($P<0.05$).

To address whether the liver X receptor (LXR) is involved in betulin induced ABCA1 up-regulation, we examined LXRα and LXRβ protein expression in RAW264.7 cells. Western blotting showed that betulin treatment (0.1, 0.5, and 2.5 μg/mL) exerted no effect on LXRα and LXRβ in RAW264.7 macrophage cells (Figure 3D).

Betulin inhibits atherosclerotic lesions in apoE$^{-/-}$ mice

To investigate the effect of betulin treatment on atherosclerosis development in apoE$^{-/-}$ mice, aortic atherosclerotic lesion areas were quantified using two independent methods, the *en face* method of the entire aortic tree and cryosection analysis of the aortic sinus. After twelve weeks of different treatments, the mice were euthanized, and *en face* aortic surface lesion areas were assessed using Sudan IV staining. The atherosclerosis in the chow diet group was not significant (Figure 4A). ApoE$^{-/-}$ mice on a high fat diet (HFD) showed markedly increased *en face* lesion areas (Figure 4A). Treatment with BT (L) and BT

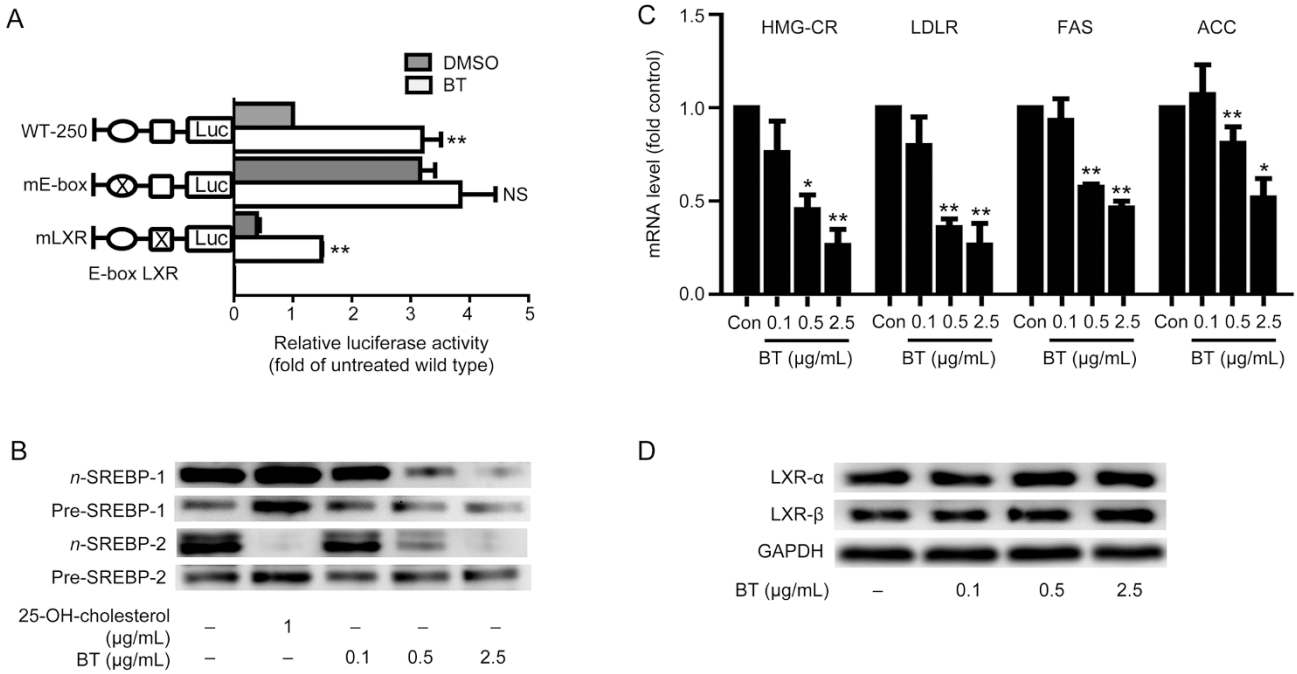

Figure 3. The effect of betulin on ABCA1 expression is mediated by the E-box motif. (A) Murine ABCA1 promoter activity was determined by luciferase activity assay. Firefly luciferase activity was normalized to *Renilla* luciferase activity and expressed as the fold change compared with the control. Luciferase activity was normalized to the intensity of the untreated wild type plasmid. (B) Protein expression of the cytosolic and nuclear forms of SREBPs was determined after betulin treatment. 25-OH-cholesterol was used as a positive control. (C) SREBP target gene expression was determined after betulin treatment. (D) Protein levels of LXRα and LXRβ were determined after betulin treatment. The data are expressed as the mean±SEM of three independent experiments. $^{*}P<0.05$, $^{**}P<0.01$ *vs* control. NS: not significant.

(H) significantly diminished the size of the *en face* aortic lesions (Sudan IV staining) compared with the HFD group (Figure 4A) by 47.02%±16.35% ($P<0.01$) and 65.35%±12.58% ($P<0.01$). Consistent with the *en face* aortas, BT (H) reduced the lesion areas in the aortic arches (Figure 4C) ($P<0.01$). Similar changes were also observed in the thoracic (Figure 4D) ($P<0.05$) and abdominal (Figure 4E) ($P<0.01$) aortas.

The aortic sinus is the area that is most susceptible to the development of atherosclerosis. We therefore further investigated lesion areas in the aortic sinus. Atherosclerosis was evaluated by quantifying the areas of ORO staining in cryosections of the aortic sinus. Betulin treatment significantly ameliorated HFD induced atherosclerosis in the aortic sinus (Figure 4F). The mean ORO staining areas were $(127.04\pm40.30)\times10^3$, $(43.40\pm10.37)\times10^3$, and $(25.18\pm5.05)\times10^3$ μm^2 for the HFD model group, BT (L) and BT (H) groups, respectively ($P<0.01$; Figure 4G).

We further investigated the effect of betulin on body weight, food intake and plasma lipid levels. Food intake and body weight were not significantly different among the groups. Compared with the HFD model group, plasma TC levels were significantly decreased in the atorvastatin (10 mg/kg) group ($P<0.01$) and the BT (H) group ($P<0.01$). Plasma LDL-c levels were significantly decreased in the atorvastatin (10 mg/kg) group ($P<0.01$) and the betulin (H) group ($P<0.01$). TG levels in the betulin (H) group were slightly decreased compared with those in the HFD model group. These data suggest that betulin treatment suppresses atherosclerosis and improves plasma lipid profiles.

Betulin up-regulates ABCA1 expression in the aortic sinus *in vivo*

Given the above observations, we investigated the macrophage content of and ABCA1 expression in the aortic sinus using immunofluorescence to determine whether betulin exerted direct effects on the aortic sinus. Representative images were shown in Figure 5A–5D, and the quantification of these results was summarized in Figure 5E and 5F. In this study, we focused on expression changes in the aortic sinuses of mice, especially on the plaques in the aortic sinuses. Therefore, we quantified the positive areas in the aortic sinuses, especially in the lesion areas, which was consistent with other research[28]. The results showed that elevated Mac-2 expression was observed in the HFD group, but low expression was observed in the betulin (L) and (H) group, indicating that macrophage-derived foam cells were widely dispersed in aortic sinus lesion areas in the HFD group. Conversely, mice treated with 40 mg/kg betulin showed a marked increase in ABCA1 in the aortic sinus ($P<0.01$), but not mice in the HFD group.

These data suggest that betulin reduces macrophage derived foam cell content and enhances ABCA1 expression in the aortic sinus, which is consistent with the *in vitro* findings.

Betulin enhances fecal cholesterol excretion in apoE$^{-/-}$ mice

To demonstrate the effects of betulin on reverse cholesterol

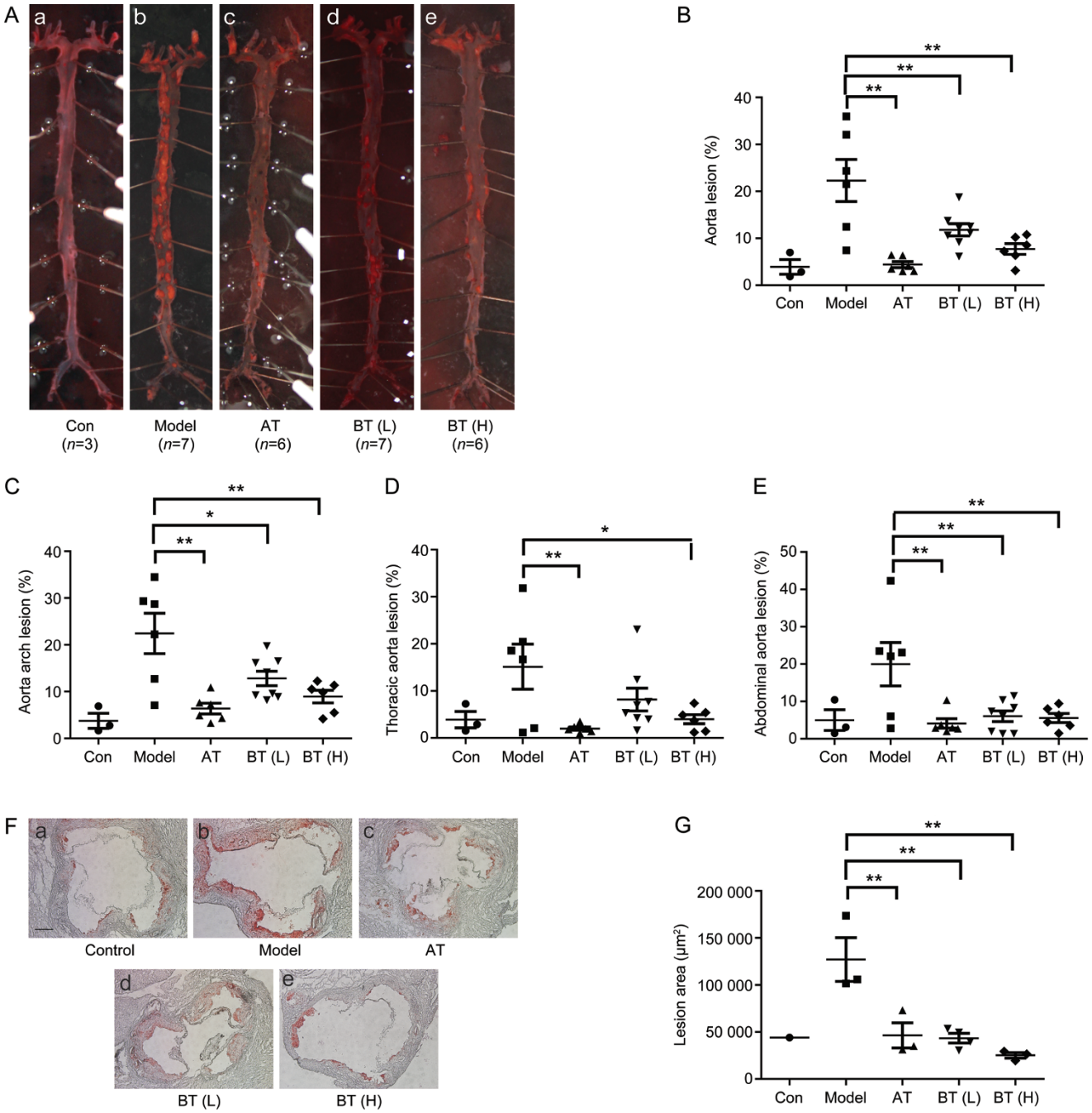

Figure 4. Betulin suppresses atherosclerotic lesions in apoE$^{-/-}$ mice. ApoE$^{-/-}$ mice were treated as described in the Methods section. Representative images of *en face* aortas (A) in each group of mice are shown (a: normal diet; b: high fat diet; c: atorvastatin; d: betulin 20 mg/kg; e: betulin 40 mg/kg). Quantitative analysis of the *en face* aorta (B), aortic arch (C), thoracic aorta (D) and abdominal aorta (E) using Sudan IV staining, calculated as the percentage of the lesion area to the total aortic area. Values are expressed as the mean±SEM. The aortic sinuses of animals, which were treated as described in the Methods section, were analyzed for atherosclerotic lesion sizes with Oil Red O staining (F). Magnification is ×50. Atherosclerotic lesion areas in the aortic sinus were quantified (G). Values are expressed as the mean±SEM. $^{*}P<0.05$, $^{**}P<0.01$ *vs* model. Scale bar=5 μm.

transport (RCT), we measured the cholesterol content in the liver, intestine and feces of the different treatment groups of apoE$^{-/-}$ mice.

As shown in Figure 6A and 6B, after 12 weeks of treatment, hepatic cholesterol decreased significantly in the BT(H) group compared with the model group, ($P<0.01$). Similar changes were also observed in the intestinal cholesterol analysis of the BT (H) group ($P<0.01$). Because plasma, liver and intestine cholesterol levels decreased significantly, we subsequently investigated whether excessive cholesterol translated into fecal excretion. The result in Figure 6C shows that cholesterol increased significantly in the feces of BT (L) and BT (H) com-

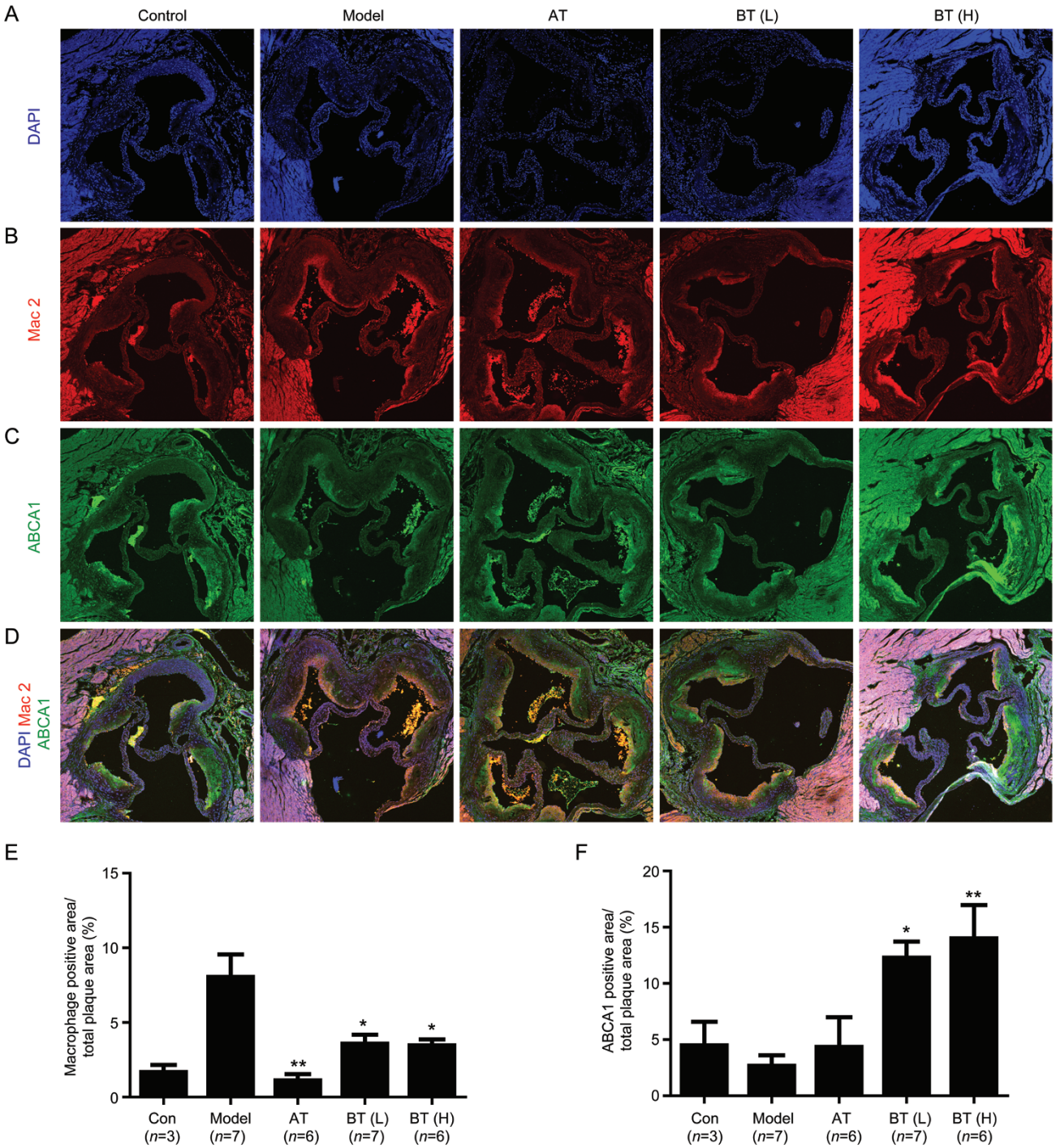

Figure 5. Betulin up-regulates ABCA1 expression in the aortic sinus *in vivo*. Frozen sections of the aortic sinuses of apoE$^{-/-}$ mice in the different treatment groups were subjected to DAPI staining (A), macrophage labeling with Mac-2 (red) (B), ABCA1 immunofluorescence staining (green) (C) and merged images (D). Staining images of the aortic sinus were obtained from three serial cryosections from each mouse. Quantitative analyses of the macrophage content (E) and ABCA1 (F) expression in the aortic sinus were conducted and calculated as a percentage of the positive area to the total lesion area. Values are expressed as the mean±SEM. $^{*}P<0.05$, $^{**}P<0.01$ *vs* model.

pared with the model group ($P<0.01$). Overall, these results demonstrated that betulin may enhance RCT *in vivo*.

Discussion

In the current study, we explored the underlying mechanisms of the anti-atherosclerotic effects of long-term betulin treatment. The results from macrophage cells showed, for the first time, that betulin enhances apoA-I and HDL mediated cholesterol efflux by promoting the mRNA and protein expression of the cholesterol transporters ABCA1 and ABCG1. Further

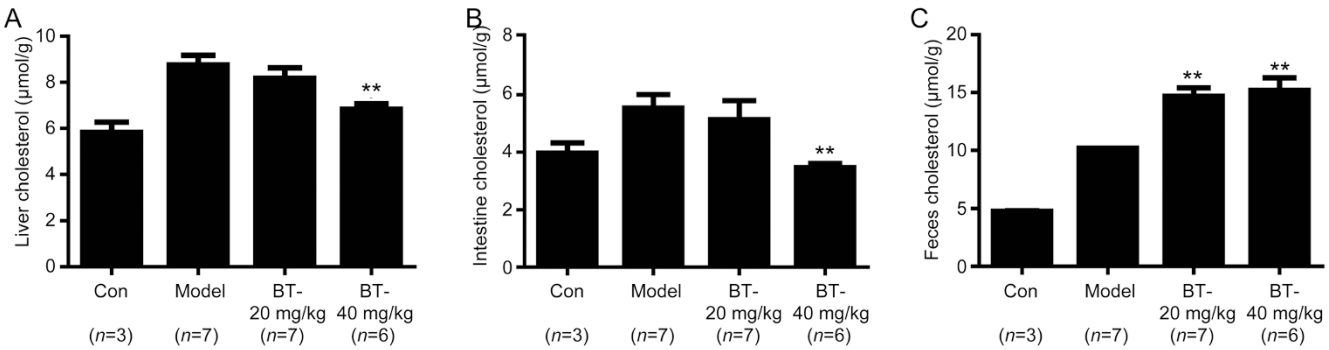

Figure 6. Betulin enhanced cholesterol fecal excretion in apoE$^{-/-}$ mice. Liver cholesterol content (A), intestine cholesterol content (B) and fecal cholesterol content (C) were analyzed to determine the effect of betulin on reverse cholesterol transport (RCT). Values are expressed as the mean±SEM. $^{**}P<0.01$ *vs* model.

studies revealed that betulin enhances ABCA1 promoter activity by suppressing the maturation of SREBPs and by inhibiting their binding to the E-box motif in the ABCA1 promoter. Consistent with the *in vitro* results, betulin up-regulates ABCA1 expression in the aortic sinuses of apoE$^{-/-}$ mice, especially in macrophages. This SREBP-regulated mechanism promotes apoA-I and HDL mediated cholesterol efflux, which is a newly defined mechanism of the atheroprotective effect of betulin.

The objective of atherosclerosis therapy is to reduce lesion progression. Lipid-accumulated macrophages contribute to the progression of atherosclerosis, thus highlighting the therapeutic potential of reversing the process[29]. Cholesterol content is modulated by two processes: cholesterol uptake[30] and cholesterol efflux[31]. We observed a significant increase in ABCA1 and ABCG1, two major cholesterol transporters mediating cholesterol efflux, upon betulin treatment in a dose-dependent manner in RAW264.7 cells and THP-1 cells (Figure 2). Consistent with the increase in cholesterol efflux transporters, betulin significantly ameliorated oxLDL-induced cholesterol accumulation in macrophages by enhancing ABCA1- and ABCG1-mediated cholesterol efflux in a dose-dependent manner (Figure 1). Recognition and uptake of oxLDL are mainly mediated by macrophage scavenger receptors, especially by CD36[30]. In the present study, we showed that betulin exerted no effect on CD36 in murine RAW264.7 cells and human monocyte THP-1 cells (Figure 2). Therefore, the probability of an oxLDL uptake process occurring is very unlikely, as it would require a large decrease in CD36 expression, which we did not observe in our model.

RAW264.7 and THP-1 are well-recognized mouse and human macrophage cell lines, respectively. They resemble primary monocytes and macrophages in morphology and differentiation properties[32, 33]. The effect of betulin on ABCA1 and ABCG1 was consistent in both cell lines (Figure 2). Primary macrophages isolated from apoE$^{-/-}$ mice may reflect the *in vivo* effects of betulin more directly. Further study is needed to demonstrate the effect of betulin on primary macrophages.

The E-box motif in the ABCA1 promoter is the recognition element for the basic helix–loop–helix leucine zipper containing proteins such as the SREBPs[34]. SREBPs (SREBP-1a, -1c, and -2) are major transcription factors activating a number of genes involved in the synthesis of cholesterol and fatty acids[34, 35]. Deletion of the E-box motif caused a 3-fold increase in transcriptional activity under basal conditions[14], and nuclear SREBP-2 down-regulates ABCA1 by binding to the E-box motif of the ABCA1 promoter[15]. In our experiments, a specific E-box binding site mutation of the ABCA1 promoter blocked the effect of betulin on ABCA1 promoter luciferase activity, suggesting the involvement of the E-box binding site in betulin-mediated effects (Figure 3A). We also observed a marked decrease in nuclear SREBP levels in RAW264.7 cells upon betulin treatment (Figure 3B). In addition, betulin inhibited SREBP target genes, such as HMG-CR, LDLR, and FAS, in macrophages (Figure 3C), HepG2 cells and liver tissues (Figure S1), confirming its specific effects on SREBPs.

ApoE, a component of LDL, is recognized by LDLR and mediates the recognition and recycling of circulating LDL[36]. Inhibition of LDLR in the liver may jeopardize the clearance of circulating LDL in the wild type mouse. However, in this study, the animal model was the apoE-deficient mouse, which is characterized by homozygous deletion of the apoE gene[37]. Therefore, the deletion of ApoE may result in the failure of LDLR- and LRP-mediated clearance of LDL[38] and result in a high level of circulating LDL cholesterol[39]. Because the clearance of LDL by apoE/LDLR recognition is absent in apoE$^{-/-}$ mice, the expression change in LDLR (Figure S1) may not affect circulating LDL levels.

Cholesterol hemostasis is maintained by cholesterol clearance and cholesterol synthesis. ApoE$^{-/-}$ mice are characterized by an impairment in the apoE/LDLR cholesterol clearance pathway[38]. Therefore, a series of genes regulating cholesterol and fatty acid biosynthesis was analyzed. As shown in Figure S1, high doses betulin (30 mg/kg) significantly inhibited the mRNA expression of HMG-CR, ACC and FAS in the liver tissues of apoE$^{-/-}$ mice ($P<0.05$). Therefore, the lipid-lowering effects (Table 2) of betulin may result from the inhibition of cholesterol and fatty acid biosynthesis, which is consistent with the results shown in Figure 3B and the concept that SREBPs are master transcription factors for cholesterol and

fatty acid biosynthesis[40].

Liver X receptors (LXRs) are another important regulator of cholesterol and fatty acid homeostasis contributing to the regulation of the gene encoding ABCA1[41, 42]. Although LXR agonists, such as GW3965[17] and T0901317[18], promote ABCA1 expression and inhibit the development of atherosclerosis in mice, they also activate SREBP-1c in the liver, leading to hypertriglyceridemia in mice due to the induction of *de novo* lipogenesis[16].

Mutagenesis of the ABCA1 promoter in the LXR binding site did not block betulin-induced effects (Figure 3A). Western blotting showed that betulin did not affect LXRα and LXRβ protein levels in RAW264.7 cells (Figure 3D), indicating that the LXR pathway was not involved in the effects of betulin on ABCA1. These results are consistent with a previous study[43] showing that betulinic acid, a derivative of betulin, is not an agonist of LXRα.

Sudan IV staining and Oil Red O staining revealed that betulin suppressed atherosclerosis in apoE$^{-/-}$ mice (Figure 4), with decreased accumulation of cholesterol in *en face* aortas and the aortic sinus. Such reductions in lesion area are similar to the results from LDLr$^{-/-}$ mice[21]. Although betulin reduced plasma TC and LDL levels in apoE$^{-/-}$ mice on a high fat diet, the plasma cholesterol concentration of these animals remained elevated comparing with that of the animals on a chow diet (Table 2). A previous study showed that this degree of hypercholesterolemia is still correlated with atherosclerosis[44]. Other mechanisms may be involved in the effect of betulin on atherosclerosis. Therefore, the direct effects of betulin on foam cell formation and cholesterol efflux were investigated in the current study.

Macrophage dysfunction and accumulation initiates atherosclerosis and promotes lesion instability[45]. To determine the effect of betulin on macrophages *in vivo*, we performed immunofluorescence experiments on cryosections of the aortic sinus from different treatment groups of apoE$^{-/-}$ mice. Consistent with the decreases in size of the atherosclerotic lesions, macrophage contents, as labeled by Mac-2, were significantly inhibited by betulin treatment (Figure 5). Moreover, we observed a marked increase in ABCA1 expression in the aortic sinus, which was induced by betulin treatment, suggesting a direct effect on the artery wall (Figure 5). By co-localizing macrophage positive areas with ABCA1 positive areas, we observed that ABCA1 was enhanced, but not only in macrophages. Further studies will be necessary to demonstrate the potential effects of betulin on other cell types.

In conclusion, suppression of the nuclear form of SREBPs by long-term treatment with betulin enhances the expression of ABCA1 and ABCG1 in macrophages and promotes cholesterol efflux *in vitro* and *in vivo*. These data should be considered additional evidence supporting the key role of ABCA1 in betulin-mediated anti-atherosclerotic effects. Our study suggests that ABCA1 up-regulation, together with SREBP suppression, may be a useful strategy for drug discovery to treat atherosclerosis. Betulin may be a promising compound for the treatment of atherosclerosis.

Author contribution

Yu-zhou GUI, Hong YAN, and Yi-ping WANG designed the research; Yu-zhou GUI, Hong YAN, Fei GAO, Cong XI, and Hui-hui LI performed the research; Yu-zhou GUI and Hong YAN analyzed the data; Yu-zhou GUI wrote the paper; Hong YAN and Yi-ping WANG revised the paper.

Supplementary information

Supplementary information is available on the website of Acta Pharmacologica Sinica.

References

1 Libby P, Ridker PM, Hansson GK. Progress and challenges in translating the biology of atherosclerosis. Nature 2011; 473: 317–25.
2 Cuchel M, Rader DJ. Macrophage reverse cholesterol transport: key to the regression of atherosclerosis? Circulation 2006; 113: 2548–55.
3 Van Eck M, Pennings M, Hoekstra M, Out R, Van Berkel TJ. Scavenger receptor BI and ATP-binding cassette transporter A1 in reverse cholesterol transport and atherosclerosis. Curr Opin Lipidol 2005; 16: 307–15.
4 Attie AD, Kastelein JP, Hayden MR. Pivotal role of ABCA1 in reverse cholesterol transport influencing HDL levels and susceptibility to atherosclerosis. J Lipid Res 2001; 42: 1717–26.
5 Yancey PG, Bortnick AE, Kellner-Weibel G, de la Llera-Moya M, Phillips MC, Rothblat GH. Importance of different pathways of cellular cholesterol efflux. Arterioscler Thromb Vasc Biol 2003; 23: 712–9.
6 Rogler G, Trumbach B, Klima B, Lackner KJ, Schmitz G. HDL-mediated efflux of intracellular cholesterol is impaired in fibroblasts from Tangier disease patients. Arterioscler Thromb Vasc Biol 1995; 15: 683–90.
7 Remaley AT, Schumacher UK, Stonik JA, Farsi BD, Nazih H, Brewer HB Jr. Decreased reverse cholesterol transport from Tangier disease fibroblasts. Acceptor specificity and effect of brefeldin on lipid efflux.

Table 2. Body weight, food intake and plasma lipids in apoE$^{-/-}$ mice fed a normal chow or high fat diet. Values are expressed as the mean±SD. $^{**}P<0.01$, mice from model (HFD) group *vs* those on a chow diet (control group). $^{\#}P<0.05$, $^{\#\#}P<0.01$ betulin treatment *vs* model (HFD) group.

Group	Body weight (g)	Food intake (g/d per 20 g bw)	TC (mmol/L)	LDL (mmol/L)	TG (mmol/L)
Control	27.33±1.53	2.20±0.12	10.42±1.48	7.58±0.80	0.78±0.38
Model	27.79±1.63	2.17±0.17	31.14±3.47**	23.14±3.02**	0.69±0.39
Atorvastatin	26.33±2.52	2.43±0.36	15.19±4.01$^{\#\#}$	10.23±2.85$^{\#\#}$	0.48±0.18
Betulin (20 mg/kg)	26.31±1.39	2.29±0.12	23.88±4.15$^{\#\#}$	18.04±3.62$^{\#}$	0.41±0.17
Betulin (40 mg/kg)	26.17±1.63	2.30±0.14	21.36±3.16$^{\#\#}$	16.75±2.77$^{\#\#}$	0.33±0.17

Arterioscler Thromb Vasc Biol 1997; 17: 1813–21.
8 Lawn RM, Wade DP, Garvin MR, Wang X, Schwartz K, Porter JG, *et al.* The Tangier disease gene product ABC1 controls the cellular apolipoprotein-mediated lipid removal pathway. J Clin Invest 1999; 104: R25–31.
9 Joyce CW, Amar MJ, Lambert G, Vaisman BL, Paigen B, Najib-Fruchart J, *et al.* The ATP binding cassette transporter A1 (ABCA1) modulates the development of aortic atherosclerosis in C57BL/6 and apoE-knockout mice. Proc Natl Acad Sci U S A 2002; 99: 407–12.
10 Aiello RJ. Increased atherosclerosis in hyperlipidemic mice with inactivation of ABCA1 in macrophages. Arterioscler Thromb Vasc Biol 2002; 22: 630–7.
11 Van Eck M, Singaraja RR, Ye D, Hildebrand RB, James ER, Hayden MR, *et al.* Macrophage ATP-binding cassette transporter A1 overexpression inhibits atherosclerotic lesion progression in low-density lipoprotein receptor knockout mice. Arterioscler Thromb Vasc Biol 2006; 26: 929–34.
12 Yvan-Charvet L, Ranalletta M, Wang N, Han S, Terasaka N, Li R, *et al.* Combined deficiency of ABCA1 and ABCG1 promotes foam cell accumulation and accelerates atherosclerosis in mice. J Clin Invest 2007; 117: 3900–8.
13 Santamarina-Fojo S, Peterson K, Knapper C, Qiu Y, Freeman L, Cheng JF, *et al.* Complete genomic sequence of the human ABCA1 gene: analysis of the human and mouse ATP-binding cassette A promoter. Proc Natl Acad Sci U S A 2000; 97: 7987–92.
14 Yang XP, Freeman LA, Knapper CL, Amar MJ, Remaley A, Brewer HB Jr, *et al.* The E-box motif in the proximal ABCA1 promoter mediates transcriptional repression of the ABCA1 gene. J Lipid Res 2002; 43: 297–306.
15 Zeng L, Liao H, Liu Y, Lee TS, Zhu M, Wang X, *et al.* Sterol-responsive element-binding protein (SREBP) 2 down-regulates ATP-binding cassette transporter A1 in vascular endothelial cells: a novel role of SREBP in regulating cholesterol metabolism. J Biol Chem 2004; 279: 48801–7.
16 Costet P, Luo Y, Wang N, Tall AR. Sterol-dependent transactivation of the ABC1 promoter by the liver X receptor/retinoid X receptor. J Biol Chem 2000; 275: 28240–5.
17 Joseph SB, McKilligin E, Pei L, Watson MA, Collins AR, Laffitte BA, *et al.* Synthetic LXR ligand inhibits the development of atherosclerosis in mice. Proc Natl Acad Sci U S A 2002; 99: 7604–9.
18 Terasaka N, Hiroshima A, Koieyama T, Ubukata N, Morikawa Y, Nakai D, *et al.* T-0901317, a synthetic liver X receptor ligand, inhibits development of atherosclerosis in LDL receptor-deficient mice. FEBS Lett 2003; 536: 6–11.
19 Jager S, Trojan H, Kopp T, Laszczyk MN, Scheffler A. Pentacyclic triterpene distribution in various plants — rich sources for a new group of multi-potent plant extracts. Molecules 2009; 14: 2016–31.
20 Yogeeswari P, Sriram D. Betulinic acid and its derivatives: a review on their biological properties. Curr Med Chem 2005; 12: 657–66.
21 Tang JJ, Li JG, Qi W, Qiu WW, Li PS, Li BL, *et al.* Inhibition of SREBP by a small molecule, betulin, improves hyperlipidemia and insulin resistance and reduces atherosclerotic plaques. Cell Metab 2011; 13: 44–56.
22 World Medical Association Declaration of Helsinki: ethical principles for medical research involving human subjects. J Am Coll Dent 2014; 81: 14–8.
23 Okamoto H, Iwamoto Y, Maki M, Sotani T, Yonemori F, Wakitani K. Effect of JTT-705 on cholesteryl ester transfer protein and plasma lipid levels in normolipidemic animals. Eur J Pharmacol 2003; 466: 147–54.
24 Smith JD, Le Goff W, Settle M, Brubaker G, Waelde C, Horwitz A, *et al.* ABCA1 mediates concurrent cholesterol and phospholipid efflux to apolipoprotein A-I. J Lipid Res 2004; 45: 635–44.
25 Huang L, Fan B, Ma A, Shaul PW, Zhu H. Inhibition of ABCA1 protein degradation promotes HDL cholesterol efflux capacity and RCT and reduces atherosclerosis in mice. J Lipid Res 2015; 56: 986–97.
26 Bijl N, van Roomen CP, Triantis V, Sokolovic M, Ottenhoff R, Scheij S, *et al.* Reduction of glycosphingolipid biosynthesis stimulates biliary lipid secretion in mice. Hepatology 2009; 49: 637–45.
27 Nicholson AC, Frieda S, Pearce A, Silverstein RL. Oxidized LDL binds to CD36 on human monocyte-derived macrophages and transfected cell lines. Evidence implicating the lipid moiety of the lipoprotein as the binding site. Arterioscler Thromb Vasc Biol 1995; 15: 269–75.
28 Rotllan N, Ramirez CM, Aryal B, Esau CC, Fernandez-Hernando C. Therapeutic silencing of microRNA-33 inhibits the progression of atherosclerosis in Ldlr$^{-/-}$ mice—brief report. Arterioscler Thromb Vasc Biol 2013; 33: 1973–7.
29 Li AC, Glass CK. The macrophage foam cell as a target for therapeutic intervention. Nat Med 2002; 8: 1235–42.
30 Kunjathoor VV, Febbraio M, Podrez EA, Moore KJ, Andersson L, Koehn S, *et al.* Scavenger receptors class A-I/II and CD36 are the principal receptors responsible for the uptake of modified low density lipoprotein leading to lipid loading in macrophages. J Biol Chem 2002; 277: 49982–8.
31 McNeish J, Aiello RJ, Guyot D, Turi T, Gabel C, Aldinger C, *et al.* High density lipoprotein deficiency and foam cell accumulation in mice with targeted disruption of ATP-binding cassette transporter-1. Proc Natl Acad Sci U S A 2000; 97: 4245–50.
32 Schmidt HH, Warner TD, Nakane M, Forstermann U, Murad F. Regulation and subcellular location of nitrogen oxide synthases in RAW264.7 macrophages. Mol Pharmacol 1992; 41: 615–24.
33 Auwerx J. The human leukemia cell line, THP-1: a multifacetted model for the study of monocyte-macrophage differentiation. Experientia 1991; 47: 22–31.
34 Brown MS, Goldstein JL. The SREBP pathway: regulation of cholesterol metabolism by proteolysis of a membrane-bound transcription factor. Cell 1997; 89: 331–40.
35 Horton JD, Shimomura I. Sterol regulatory element-binding proteins: activators of cholesterol and fatty acid biosynthesis. Curr Opin Lipidol 1999; 10: 143–50.
36 Mahley RW. Apolipoprotein E: cholesterol transport protein with expanding role in cell biology. Science 1988; 240: 622–30.
37 Zhang SH, Reddick RL, Piedrahita JA, Maeda N. Spontaneous hypercholesterolemia and arterial lesions in mice lacking apolipoprotein E. Science 1992; 258: 468–71.
38 Knowles JW, Maeda N. Genetic modifiers of atherosclerosis in mice. Arterioscler Thromb Vasc Biol 2000; 20: 2336–45.
39 Plump AS, Smith JD, Hayek T, Aalto-Setala K, Walsh A, Verstuyft JG, *et al.* Severe hypercholesterolemia and atherosclerosis in apolipoprotein E-deficient mice created by homologous recombination in ES cells. Cell 1992; 71: 343–53.
40 Goldstein JL, DeBose-Boyd RA, Brown MS. Protein sensors for membrane sterols. Cell 2006; 124: 35–46.
41 Repa JJ, Turley SD, Lobaccaro JA, Medina J, Li L, Lustig K, *et al.* Regulation of absorption and ABC1-mediated efflux of cholesterol by RXR heterodimers. Science 2000; 289: 1524–9.
42 Venkateswaran A, Laffitte BA, Joseph SB, Mak PA, Wilpitz DC, Edwards PA, *et al.* Control of cellular cholesterol efflux by the nuclear oxysterol receptor LXR alpha. Proc Natl Acad Sci U S A 2000; 97: 12097–102.
43 Jayasuriya H, Herath KB, Ondeyka JG, Guan Z, Borris RP, Tiwari S, *et al.* Diterpenoid, steroid, and triterpenoid agonists of liver X receptors from diversified terrestrial plants and marine sources. J Nat Prod 2005; 68: 1247–52.
44 Getz GS, Reardon CA. Diet and murine atherosclerosis. Arterioscler Thromb Vasc Biol 2006; 26: 242–9.
45 Schrijvers DM, De Meyer GR, Herman AG, Martinet W. Phagocytosis in atherosclerosis: molecular mechanisms and implications for plaque progression and stability. Cardiovasc Res 2007; 73: 470–80.